Australian Journal of Basic and Applied Sciences, 5(10): 913-925, 2011
ISSN 1991-8178

Geochemical Constrain on the Early Cretaceous, OIB-type Alkaline Volcanic Rocks in Kojor Volcanic Field, Central Alborz Mountain, North of Iran.

[1]M.R. Ansari, [2]M. Vossoughi Abedini, [3]A. Darvish Zadeh, [4]S.J. Sheikhzakariaee, [5]Z. Hossein mirzaee Beni

[1]PhD Student Department of Geology, Science and Research Branch, Islamic Azad University, Teheran, Iran.
[2]Geological Department, Faculty of Science, University of Shahid Beheshti, Teheran, Iran.
[3]Geological Department, Faculty of Science, University of Teheran, Teheran, Iran.
[4]Assistant Professor in Department of Geology, Science and Research Branch, Islamic Azad University, Teheran, Iran.
[5]Young Research Club, Khorasgan (Isfahan) Branch, Islamic Azad University, Isfahan, Iran.

Abstract: The Kojor volcanic field (KVF), North of Iran contains a number of intra-continental alkaline volcanic range situated on central Alborz Mountains, formed along the localized extensional basins developed in relation with the lithospheric thinning and Cretaceous compersional processes. The volcanic suite comprises the extracted melt products of adiabatic decompression melting of the mantle that are represented by small-volume intra-continental plate volcanic rocks of alkaline basalts and their evaluated Rocks with compositions representative of mantle-derived, primary (or near-primary) melts. Trace element patterns with significant enrichment in LILE, HFSE and REEs, relative to Primordial Mantle. Trace element variations of individual basaltic rocks are characterized by an increase in incompatible elements and MgO, with decreasing SiO2, as melt production proceeds. They are mainly alkaline basalt. Most of these rocks display overlapping primitive Mg-numbers, Cr and Ni contents, steep chondrite-normalized rare earth element patterns (La/Yb CN = 6.46–19.26) and an overall enrichment in incompatible elements. The existence of distinct primary magmas is also indicated by heterogeneity in highly incompatible element ratios (e.g. Zr/Nb,La/Nb). Trace element modelling indicates that the magmas were generated by comparably variable degrees of partial melting of different garnet lherzolite and a heterogeneous asthenospheric mantle source.

Key words: Alborz; Iran; garnet lherzolite; partial melting.

INTRODUCTION

Continental volcanic rocks can provide important information about paleo-geodynamic settings and the processes controlling the geochemical evolution of the sub-continental mantle. However, systematic studies of igneous rocks and the chemical composition of the mantle underlying the continental plate are few in number. Alkaline basalt occurs in a variety of geologic and tectonic settings and their detailed study in space and time helps in various ways to understand several geological events. Thought to be an integral part of continental rifting and / or local extensional regime occur in continental fragments. They also serve as major conduits for magma transfer from mantle to the upper crust and constitute a common expression of crustal extension. Another important point is that the continental volcanic rocks have their origin related in some way to the uprise of hot mantle plumes that ultimately may lead to rifting and, ultimately, continental break-up. The mantel source of alkaline basalt is very common and the study of these rocks is an important tool in understanding the evolution of the sub-continental lithosphere and asthenospheric. The magmatic rocks of Alborz mountain range also have different petrological nature. These cretaceous basaltic rocks are well exposed around central part of Alborz mountain range. This rock is known as Javherdasht and Javaherdeh cretaceous volcanic field, (GSI, 1997; Haghnazar *et al* 2009) Amlash cretaceous volcanic field and Central Alborz. These rocks consist of a variety of alkaline and basaltic rocks. Most previous workers (GSI, 1997; Haghnazar *et al* 2009) have given their attention to examine the alkaline rocks only and no petrological and geochemical work is available on these basic rocks. First hand petrological and geochemical information on volcanic rocks of Kojor volcanic field and a suggestion on their possible origin have been resented in the present paper. The detailed petrological and geochemical studies of these rocks are important because most of these follow the direction of major structural features, particularly the deep faults present in the region. Space and time correlation of these rocks with other volcanic rocks suite derived from the sub Alborz mantle plume will help in understanding the continental break-up during the Cretaceous time.

Corresponding Author: M.R. Ansari, PhD Student Department of Geology, Science and Research Branch, Islamic Azad University, Teheran, Iran.

Geological setting:

The Alborz mountain chain extends for several hundreds of kilometres between the Caspian Sea and the Iranian Plateau (Fig. 1b). The belt is the result of different tectonic events: from the Late Triassic Cimmerian orogeny, resulting from the collision of the Iranian block with Eurasia, to the present day stage of intracontinental deformation related to the convergence between the Arabian and Eurasian plates. Important large-scale features of the belt consist in the lack of an axial metamorphic zone and in the absence of deep crustal roots (crustal thickness is 35 km, according to (Tatar *et al*., 2002), which is apparently in contrast with the present day elevation of the belt (several summits over 4000 m) which was achieved since Late Miocene (Axen *et al*., 2001). The oldest compressional event recorded in the area is the Cimmerian orogeny, which affected the Eurasian margin from Turkey to Thailand. It was chiefly caused by the early Mesozoic collision of several microplates detached from Gondwana. According to palaeogeographic reconstructions (Stocklin, 1974; Stampfli *et al*., 1991; Saidi *et al*., 1997; Besse *et al*., 1998; Gaetani *et al*., 2000; Stampfli and Borel, 2002), the Iranian microplate was the first block to collide with Eurasia during Middle-Late Triassic forming the Eo-Cimmerian orogen. This event is recorded by a low-angle regional angular unconformity (Stocklin, 1974; Jenny and Stampfli, 1978) along the northern margin of the Iranian plate, sealed by the Upper Triassic-Jurassic Shemshak Formation (Assereto, 1966a; Seyed-Emami, 2003). A Permo-Triassic accretionary-subduction complex marking the Paleotethys suture between the Turan and the Iranian plate has been recognized in the Mashad and Torbatjam regions to the east (Ruttner, 1993). Tentatively traces the Paleotethys suture westward across the Gorgan region to the Talesh mountains (western Alborz), where metamorphic nappes (Clark *et al*., 1975; GSI, 1997) are unconformably covered by the Shemshak Formation. The record of the Eo-Cimmerian orogeny is less evident in the central part of the Alborz. The Upper Triassic succession is almost continuous (Ghasemi-Nejad *et al*., 2004) and is marked by a sudden change in sedimentation, from shallow sea carbonates to silicilastic sandstones, suggesting that central Alborz was located south of the main suture zone and then behaved as a stable foreland region during the collision.

Geological Setting of the Central Alborz:

The stratigraphic succession of the central Alborz (Assereto, 1966b) spans the whole Phanerozoic, Precambrian and Cambrian succession is represented by coastal sandstones and dolostones, with continental deposits in the Early Cambrian. Ordovician and Silurian are poorly represented, whereas the Devonian- Middle Triassic succession and consists of predominantly shallow marine carbonates intercalated with basaltic lava flows, evolving to a widespread carbonate platform sedimentation in the Triassic (Elika Formation). The latest Precambrian to Middle Triassic succession is unconformably covered by the Shemshak Formation, up to 4000 m thick, deposited after collision of the Iran microplate to the Eurasian margin. The age of the base of the Shemshak Formation is diachronous, being Late Triassic in the central Alborz and Early to Middle Jurassic to the north toward the Caspian Sea (Clark *et al*., 1975; Seyed-Emami, 2003; Ghasemi-Nejad *et al*., 2004; Fursich *et al*., 2005). This formation consists of continental sandstones, shale and coal passing upward to shallow marine deposits blanketing the Eo-Cimmerian orogen and its foreland. The Eo-Cimmerian unconformity is particularly evident in the Shemshak area, where the basal beds of the formation lie directly on the Permo-Carboniferous units. The shallow water Marine Middle Jurassic–Early Cretaceous carbonates and clastics were followed by early Cretaceous carbonates, basaltic and andesitic volcanic across large parts of the Alborz such as Chaloos formation and Tizkuh formation, which is irregularly preserved and locally folded (Guest *et al*., 2007). The Kojor early cretaceous volcanic field is considered a member of Chaloos formation and is located in central part of Alborz mountain ranges. Kojor volcanic alkali basalt is a large composite of the above mentioned volcanic suite which is consist of mainly Olivine basalt-Andesite Basalt, Dolerite, and subordinate pyroclastic materials (GSI. 1997).

Research Methodology:

Sixteen samples were collected from volcanic outcrops in the Kojor area, representing the entire early cretaceous sequence of the central Alborz range. These samples were prepared for analysis major and trace elements and determined by inductively coupled plasma atomic mass spectrometry (ICP-AMS) at ACME lab, Vancouver, Canada, by VAN10005683.1 and VAN10006800 file number with 4A, 1F-MS and 1T-MS full suite packages.

Results:

Petrography:

The petrography of the Kojor Volcanic rocks Field (KVF) (fig. 1a), along with the geology and the contemporaneous volcanic rocks in vary part of central Alborz mountain has been previously described by (GSI, 1997; Haghnazar *et al* 2009).

Most of samples have composition range between alkaline olivin Basalt – Trachyandesite Basalt and some samples are hypabyssal doleritic rocks

An overall consideration of the investigated basic volcanic rocks indicates that primary mineralogy in the alkali basalts is composed of olivine + plagioclase + clinopyroxene (pinkish Ti-augite) ± brown amphibole (xenocryst) + opaque oxides (e.g. Titanomagnetite), whereas the secondary mineral phases are represented by serpentine + epidote + chlorite + calcite.

Major and trace element chemistry:

The lavas from both Kojor volcanic field (KVF) are a strongly alkaline series of volcanic rocks, with almost all samples plotting in the alkali basalt and trachybasalt fields on a total alkalis (K2O+Na2O) vs. silica (SiO2) classification diagram of Le Bas *et al*. (1986) (Fig. 2). The alkaline rocks are mainly, sodic (Na2O/K2O=2.9–5.67) and have high Mg# [cation proportion]

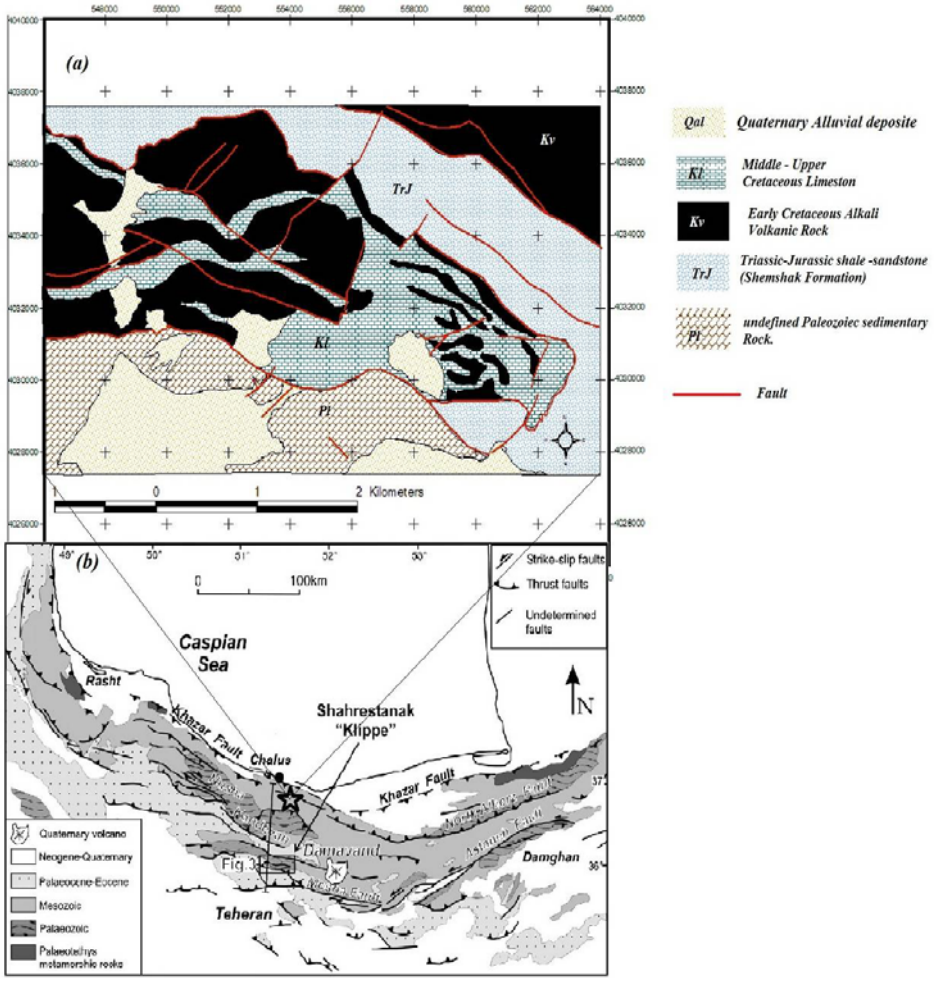

Fig. 1: (a) Simplified geological map of the Kojor area, from GSI.(1997)and our own observations.(b) Tectonic map of the Central Alborz, modified from Allen *et al*. (2003).(Zanchi *et al*., 2006).

Mg/ (Mg+Fetotal)](29.7– 64.7) and high MgO (4.4–11.4 wt.%) over a range of SiO2 content from 44.7 to 53.3 wt.%. The analyzed samples have moderate Ca (7.4–11.03 wt.% CaO) and high Al (13.8–17.5 wt.% Al2O3) contents and their Cr and Ni concentrations range variably from 41 to 170 ppm and from 97 to 293 ppm, respectively. On the Zr/TiO2 vs. Nb/Y diagram of Winchester and Floyd (1977), the KVF rocks fall in alkaline basalt – basanite field (Fig. 3). Although, rock types and whole-rock chemical compositions indicate that they are closer to primary melt compositions the alkaline rocks have almost straight and relative to chondrite normalized (CN indicates chondrite normalized) REE pattern with near-constant concentration ratios. The absolute REE abundances increasing with decrease SiO2 content. (Fig. 8) All samples have REEs enriched patterns on chondrite-normalized REE plots. The KVF lavas also have all the classic enrichments in LILE, HFSE and REEs (e.g., relative to the average Primordial mantle normalizing values) that characterize basalts from intraplate continental and oceanic island basalt settings (Fig. 4). These rocks also display prominent

negative Rb, Hf and slightly k, Ce, U anomalies and shown Nb, Pb and Zr positive anomalies. Primitive mantle normalized incompatible trace element patterns (Fig. 5) are similar to those of ocean island basalts (OIB) (Fig. 6), with strong enrichment in most highly incompatible elements. This enrichment is stronger in the alkali basalts than in the trachyandesite basalts. Alkali olivine basalts to trachy andesites have, respectively, the highest and lowest REE concentrations. The REE patterns have slight slope through the middle to heavy REE, In a N-MORB-normalized (Sun and McDonough1989) trace element plot (Fig. 7).The REE show a continuous decrease of normalized concentrations from La to Yb (Fig. 8), with (La/Yb) CN ratios of 6.46–19.26 in the alkali basalts. Concentrations of heavy REE (HREE) in all KVF basalts are lower than in typical mid-ocean ridge basalt (N-MORB). All KVF basalts show prominent anomalies in primitive mantle normalized trace element diagrams (Fig. 4). These include positive anomalies in Ba, Nb, Sr, P and Zr, and negative anomalies in Rb and K. The positive P, Ba and Nb anomalies and negative Rb,K anomalies are more prominent in the alkalin basalt than in the trachyandesites basalts . In addition, this rocks show negative anomalies of Rb, K and U and also positive Th anomalies. (Fig. 5)

Tectonic setting:

Meschede (1986) showed that within-plate alkaline basalt and E-MORB could be identified without ambiguity on the triangular plot of Zr–Nb–Y, which is also confirmed by Rollinson., 1993; Dicheng Zhu *et al* ., 2007.

Table 1: Major (wt %) and trace element (ppm) concentration of chemical composition of the investigated from KVF alkali basalt.

Sample	ABS69	ABS1	ABS14	ABS68	ABS5	ABS15	ABS2	ABS3	ABS7	ABS48	ABS26	ABS4	ABS53	ABS16	ABS67	ABS13
SIO2	46.37	44.752	48.492	46.89	45.436	53.322	47.108	46.527	47.66	46.031	45.07	46.085	46.331	45.131	46.418	45.742
TiO2	1.935	2.209	1.864	2.267	2.226	1.881	2.166	1.785	2.22	2.184	2.356	1.62	2.118	2.109	2.005	1.811
Al2O3	16.126	15.251	15.617	16.06	16.857	13.828	17.121	15.734	17.49	16.204	15.233	15.043	15.123	15.722	16.873	15.393
FeO	10.853	11.057	10.761	10.875	11.816	10.374	10.568	11.616	13.42	9.831	10.511	11.245	11.101	10.153	10.484	11.834
Fe2O3	1.913	1.953	1.897	1.92	2.079	1.826	1.86	2.049	2.367	1.713	1.855	1.985	1.956	1.788	1.845	2.09
MnO	0.245	0.181	0.178	0.22	0.126	0.143	0.164	0.137	0.139	0.385	0.256	0.16	0.205	0.235	0.202	0.182
MgO	9.652	9.691	6.083	7.327	6.617	5.512	4.442	7.19	3.138	8.696	10.202	11.384	10.55	9.778	8.916	8.886
CaO	9.652	11.073	10.793	10.732	11.028	9.241	11.631	11.02	7.435	10.159	10.386	9.125	8.384	11.058	9.706	10.792
Ce	28.3	63.8	42.8	34.0	45.9	35.7	49.7	41.4	48.0	67.1	62.3	36.5	43.1	90.5	31.2	32.5
Nd	18.5	35.9	21.6	22.4	26.9	21.2	23.9	26.8	22.1	36.8	39.2	22.2	25.5	45.8	19.5	19.3
Sm	4.1	5.6	3.9	4.5	5.0	4.0	4.4	4.6	4.1	6.2	6.7	4.4	4.8	7.0	4.1	4.0
Eu	1.3	1.8	1.4	1.6	1.8	1.4	1.6	1.5	1.5	1.9	2.1	1.4	1.6	2.1	1.5	1.4
Gd	4.3	5.7	4.1	5.1	5.9	4.4	5.0	5.0	4.7	6.3	6.2	4.5	5.1	6.5	4.4	4.2
Tb	0.6	0.8	0.6	0.7	0.8	0.6	0.7	0.8	0.7	0.8	0.8	0.7	0.7	0.9	0.7	0.6
Dy	3.8	4.8	3.9	4.5	5.1	3.9	4.7	4.8	4.1	4.8	5.1	4.5	4.5	5.1	4.3	3.9
Ho	0.7	0.9	0.7	0.9	0.9	0.8	0.8	0.9	0.8	0.9	0.8	0.8	0.9	0.9	0.7	0.7
Er	1.8	2.2	1.7	2.2	2.6	1.9	2.2	2.5	.1.9	2.2	2.2	2.1	2.1	2.4	2.0	1.9
Tm	0.2	0.3	0.2	0.2	0.3	0.3	0.3	0.3	0.2	0.3	0.3	0.3	0.3	0.3	0.2	0.2
Yb`	1.6	1.9	1.6	1.8	2.2	1.7	1.7	2.4	1.6	1.9	1.9	2.0	2.0	2.1	1.7	1.7
Lu	0.2	0.3	0.2	0.3	0.3	0.2	0.2	0.3	0.2	0.3	0.3	0.3	0.2	0.3	0.2	0.2
Y	17	22	18	20	22	20	21	22	20	21	21	20	20	23	18	17
Ta	1.2	2.8	1.4	1.3	1.8	1.4	1.7	1.5	1.6	3.2	3.3	1.3	1.5	3.8	1.3	1.3
Hf	2.61	4.28	2.15	3.31	3.16	2.27	2.61	3.62	2.51	4.92	4.61	3.11	3.31	4.08	2.86	2.57
U	0.4	1.0	0.7	0.4	0.9	0.4	0.6	0.6	1.5	0.9	0.7	0.6	0.4	1.6	0.3	0.5
Th	2.0	4.9	2.5	2.0	3.0	2.2	2.8	3.2	2.7	4.3	3.4	2.2	2.3	8.4	2.0	1.8
V	60	71	90	71	71	143	147	28	264	65	89	29	73	87	79	72
Sc	1.7	2.6	19.3	2.2	3.7	15.8	12.5	2.6	18.6	1.9	2.4	2.4	2.2	3.2	3.9	2.6
Ga	9.3	9.3	10.7	8.6	9.3	9.2	9.3	8.0	9.1	9.5	10.6	8.8	11.5	10.5	9.3	9.3
Cs	<0.04	0.15	<0.04	0.04	0.12	0.15	0.07	0. 14	0.08	0.21	0.45	0.34	0.52	0.47	0.10	0.32
Ce	28.3	63.8	42.8	34.0	45.9	35.7	49.7	41.4	48.0	67.1	62.3	36.5	43.1	90.5	31.2	32.5
Pb	1.43	5.78	2.16	1.40	1.74	2.17	2.35	3.81	2.93	2.53	3.06	2.82	1.92	6.07	1.48	1.70
Li	7.4	8.6	3.5	6.9	3.6	2.9	1.1	2.3	1.3	20.5	11.0	8.7	10.4	8.8	9.1	5.3
Pb2O4	0.01	0.10	0.02	0.01	0.02	0.02	0.02	0.04	0.03	0.02	0.03	0.03	0.02	0.05	0.01	0.02
Pb2O6	0.27	1.89	0.34	0.29	0.35	0.38	0.44	0.74	0.63	0.35	0.48	0.45	0.36	0.90	0.31	0.35
Pb2O7	0.23	1.64	0.28	0.23	0.29	0.34	0.39	0.60	0.50	0.32	0.44	0.43	0.33	0.72	0.22	0.31
Pb2O8	0.6	4.08	0.68	0.59	0.75	0.8	1.02	1.5	1.21	0.8	1.06	1.03	0.79	1.85	0.55	0.74

The Zr–Nb–Y diagrams (Fig. 9a) illustrate that the KVF basalts are characteristic of within-plate alkaline basalts, which to a large extent resemble the representative OIB (Sun and McDonough, 1989).

Generally, basaltic lavas in a continental rift setting is associated with a mantle plume, the asthenosphere, the lithospheric mantle and continental crust (Sun and McDonough, 1989). Therefore, key to study the Petrogenesis of mafic rocks is to identify the relative contributions made by mantle plumes, the normal asthenosphere, the lithospheric mantle and the continental crust. Increasing Zr/Y ratios in contrast Zr variation of KVF basalts are comparable to increase in Zr concentration (Fig. 9b). The Zr/Y ratios, reflected relatively high values owing to higher incompatibility of Zr compared to Y in mantle phases (e.g. Pearce and Norry 1979; Pearce 1980;Nicholson and Latin 1992; Kaan *et al*., 2009). Therefore, the KVF rocks could have been generated by varying degrees of melting. It must also be noted that amphibole fractionation may have accounted for a small increase in Zr/Y ratios (Kaan *et al*., 2009) high Zr/Y values of KVF samples (Zr/Y = 6.5–11.4) may suggested their derivation from enriched mantle sources or possible contribution of a mantle plume (OIB, Zr/Y

= 9.66, E-MORB = 3.32; Sun and McDonough, (1989) Or derivation from mantel metasomatized and/or by vary degrees of low fusion . The Zr/Nb values (Zr/Nb = 2.11–5) also support this suggestion. On the other hand, considerable high Zr/Nb values (Zr/Nb = 28.9–43.4) together with relatively low Zr/Y ratios may provide the contribution of depleted mantle during their generation (MORB, Zr/Y = 2.64, Zr/Nb = 31.8; Sun and McDonough (1989). lowest Y/Nb values (Y/Nb = 0.23–0.74) may be related to the involvement of enriched mantle sources and considered the garnet is a present phase in the source. The existence of residual garnet results in depletion of HREE relative to LREE because of the strong retention of HREE in garnet (e.g. Wilson 1989; Spath *et al*. 1996).

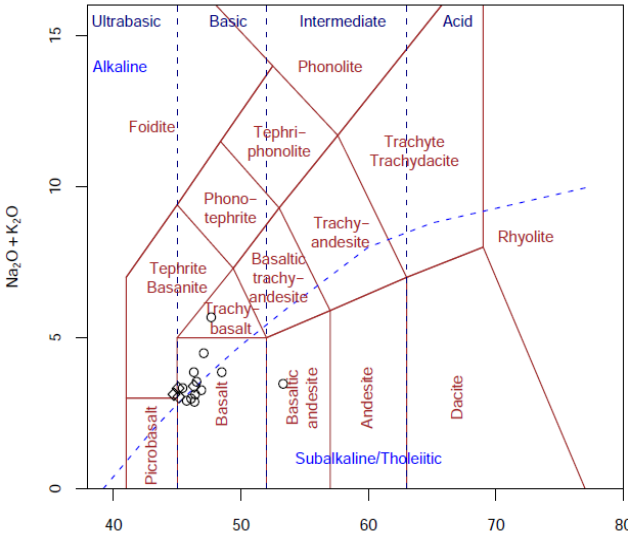

Fig. 2: Classification of the KVF alkali basalt samples in the TAS diagram after Le Bas *et al*. (1986) with alkaline^sub-alkaline magma series.

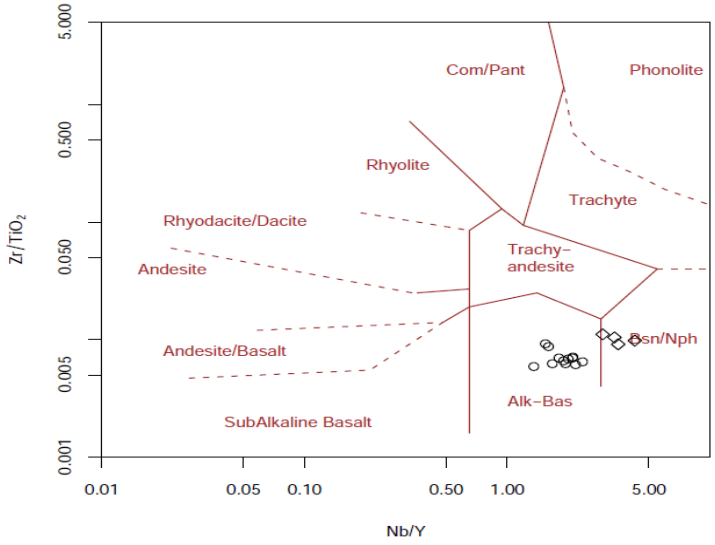

Fig. 3: Nb/Y–Zr/TiO2 diagram of Winchester and Floyd (1977) showing the alkaline basalt affinity of the KVF volcanic rocks.

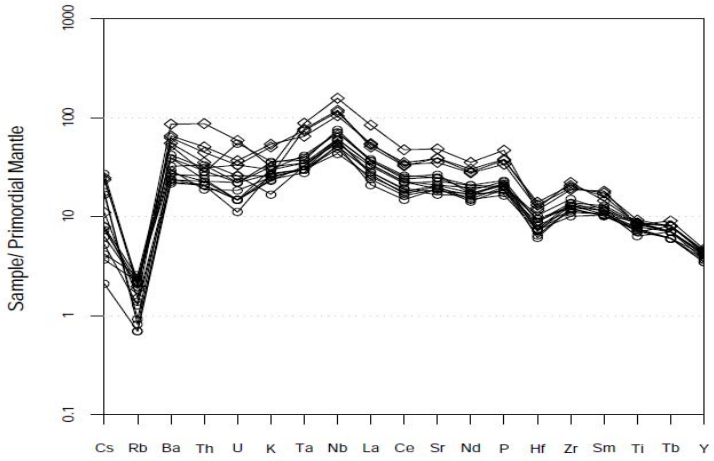

Fig. 4: Primordial mantle-normalized trace element diagrams showing the compositions of KVF alkali basalt. Primitive mantle normalizing composition is from Sun & McDonough (1989).

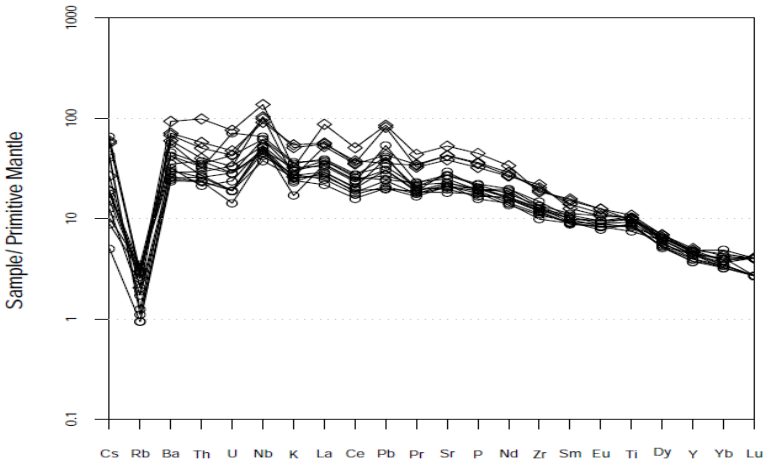

Fig. 5: Primitive mantle-normalized trace element diagrams showing the compositions of KVF alkali basalt. Primitive mantle normalizing composition is from Sun & McDonough (1989).

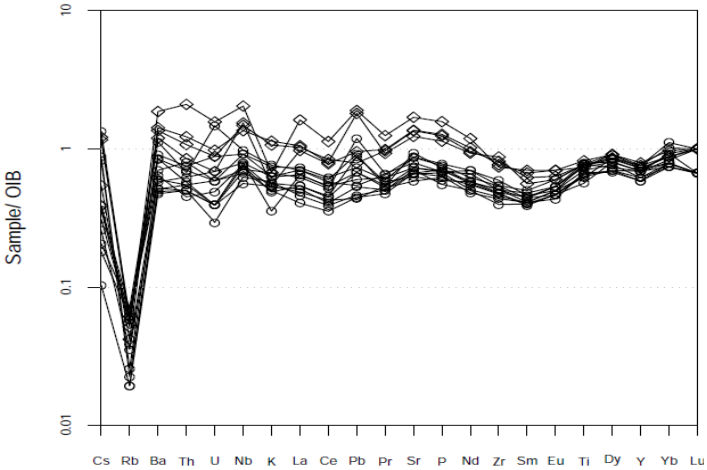

Fig. 6: OIB normalized trace element diagrams showing the compositions of KVF alkali basalt. Primitive mantle normalizing composition is from Sun & McDonough (1989).

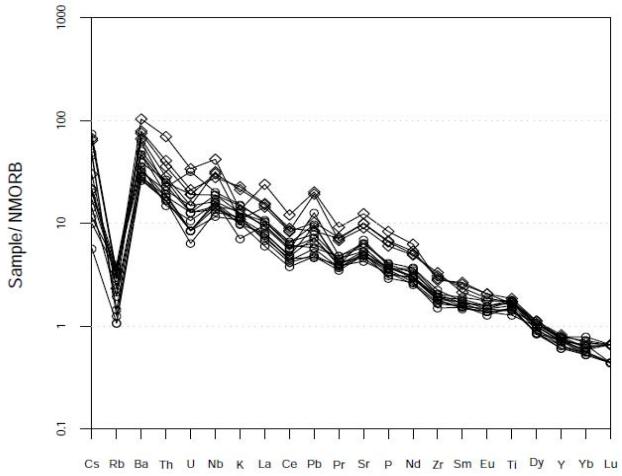

Fig. 7: N-MORB normalized multi element patterns diagrams for KVF alkali basalt. Normalizing values are from (Sun and McDonough1989).

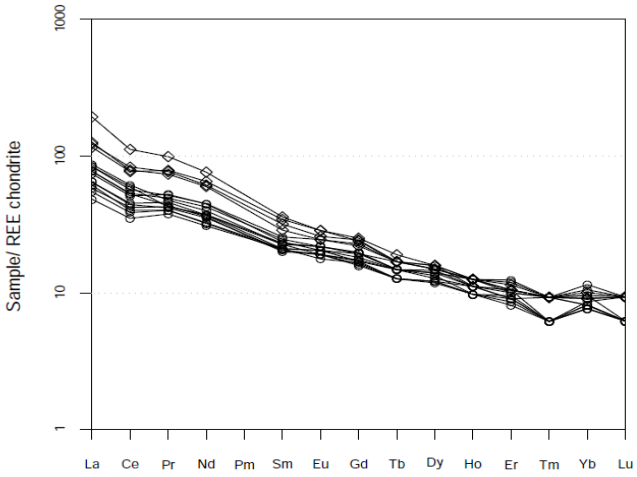

Fig. 8: Chondrite-normalized REE diagrams for KVF alkali basalt. Normalizing values are from (Boynton1984).

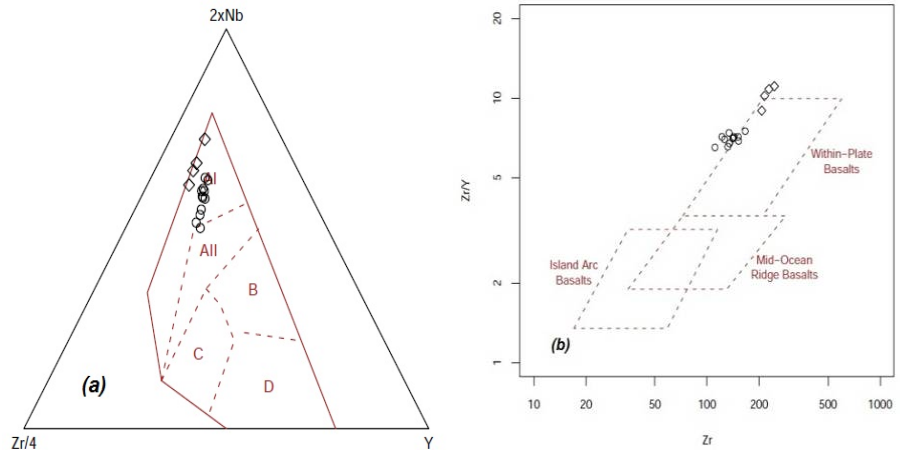

Fig. 9: (a) Nb–Zr–Y discrimination diagram (Meschede, 1986) for the KVF alkali basalts. The fields are defined as follows: AI, within-plate alkali basalts; AII, within-plate alkali basalts and within-plate tholeiites; B, E-type MORB; C, within-plate tholeiites and volcanic-arc basalts; D, N-type MORB and volcanic-arc basalts.(b) Tectonomagmatic discrimination plots of thestudied sample KVF alkali basalts after Pearce and Norry (1979).

As indicated by high partition coefficients of those elements (e.g. Green *et al*. 1989; Jenner *et al*. 1994). The alkaline basalts display considerable depletion HREE compared to LREE ([La/Yb] CN suggesting the presence of garnet as a residual phase in the source of these basalts. It must also be noted that [Tb/Yb] CN values of KVF basalts ([Tb/Yb]CN = 1.41– 1.86, respectively) are somewhat in agreement with those of alkaline basalts from Hawaii ([Tb/Yb]CN = 1.89–2.45), which are also thought to be derived from a garnet-bearing source. However high Dy/Yb ratios displayed by alkaline basalts (Dy/Yb = 1.3–1.79) with respect to that of chondrite (Dy/Yb = 1.49; Sun and McDonough 1989), on the other hand, may suggest a garnet-bearing lherzolite source for the derivation of these alkaline basalts.Taking the geochemical discrimination diagrams into account it is concluded that the KVF basalts were formed in a continental extensional setting, although the volcanic rocks have similar geochemical features to OIB.

Petrogenesis of Alkaline Rocks and Mantle Process:

The foregoing description suggests that the KVF alkali basalts may have been derived from mantle source materials resembling those of many oceanic island basalts. This will be further corroborated in the following discussion. Nb, Th and La are immobile elements and seawater alteration would not change the Nb/ Th and La/ Nb ratios (Dicheng Zhu *et al*., 2007). These ratios are also not susceptible to magma processes because they have similar partition coefficient (Li., 1993; Dicheng Zhu et al., 2007). The island arc basalts, MORB and OIB can be distinguished well by La/ Nb–La diagram (Fig. 10). Obviously, the KVF alkali basalts all plots within the OIB field is shown in the following diagram (Fig. 10).

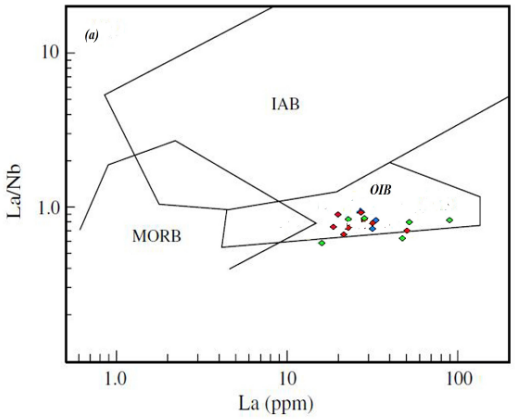

Fig. 10: Trace element discrimination diagrams for the tectonic setting of Cretaceous basaltic rocks in KVF, North of Iran, La vs. La/Nb diagram after (Li,1993) showing characteristics of an OIB-type source. The fields are defined as follows: IAB, Island-arc basalts; MORB, mid-ocean ridge.

OIB Basalts; oceanic island basalts:

On the other hand, Shaw *et al*, 2003; Weinstien *et al*, 2006 argued that alkali basaltic magmas are formed by relatively shallow melting of lithospheric mantle. A lithospheric mantle source seems also not to be necessary for the KVF alkali basalts (Fig. 11), although, OIB-type characteristics exert a strong control on the trace element systematic of these basalts. The (Yb) CN-(La/Yb) CN diagram (Fig.11) illustrates the approximate melt compositions of the KVF alkali basalts, which fall between the garnet lherzolite field non-modal fractional melting curves, suggesting that the magmas were formed by the melting of garnet lherzolite and we find no evidence for spinel lherzolite melting. The notable fractionation between the LREE and HREE ((La/Yb)CN = 6.46–19.26) and the high (Yb)CN(7.65–11.48) of the KVF alkali basalts correspond a low degree between(5-12%) partial melting of garnet lherzolite .Trace element ratios such as Nb/Th and Ti/Yb are helpful in distinguishing crustal contamination from interaction with sub-continental lithospheric mantle, because these ratios are very sensitive to the crustal contamination of mantle-derived magmas (Li *et al*., 2002; Dicheng Zhu *et al*., 2007).

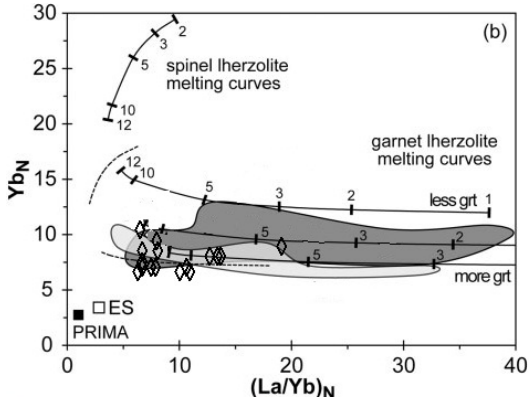

Fig. 11: Diagrams of chondrite-normalized La/Yb vsYb for uncontaminated Syrian HAS lavas. Additionally, data fields are from Weinstein *et al*. (2006) and Shaw *et al*. (2003) for the Israeli and Jordanian HAS lavas, respectively. Also shown are melting curves for non-modal batch melting of garnet and spinel lherzolites of PRIMA compositions (dashed lines) and enriched source compositions (representing mantle enriched with 15% of a 2_5% melt from 0_5% depleted mantle of PRIMA composition) with variable amounts of garnet (continuous lines); the numbers give the degree of melting. PRIMA and chondrite values are from McDonough & Sun (1995).

In the Ti/Yb vs.Nb/Th plot (Fig. 12), most KVF alkali basalts show relatively uniform Ti/Yb and Nb/Th ratios, close to those of the representative alkaline OIB (Sun and McDonough, 1989), and shown lesser-contaminated basalts plot with sub-continental lithospheric mantle and/or the lower crust. It is well known that there is no sub-continental lithospheric mantle beneath Hawaii, thus the Ti/Yb vs. Nb/Th plots seem imply that sub-continental lithospheric mantle and/or lower crust components were affected to generation of the KVF alkali basalts. Most of authors(e.g., Mehdizadeh *et al*, 2002 ; Liotard *et al*, 2008; Taki *et al*,2009) suggested magmatism in Alborz mountains related to an enrichment event must have modified the mantle source prior to the initiation of partial melting. Metasomatic agents affecting the mantle sources may have included either volatile-rich partial melts or H2O–CO2 fluids that originated from the dehydration or partial melting of subducted slabs (Menzies and Hawkesworth, 1987; Hawkesworth *et al*., 1990) or from plume heads (McKenzie, 1989; Tainton and McKenzie, 1994). A number of geochemical studies on Damavand dormant volcano and other basaltic rocks in central Alborz shown Nb, Ta, and Ti depletions, LILE enrichment, positive Ba and Pb anomaly as well as their similarity to the shoshonitic series lavas were regarded as a ubiquitous subduction zone signature by Mehdizadeh *et al*, 2002; Liotard *et al*, 2008; Taki *et al* 2009 .These authors also indicated that the enrichment event was related to subduction of either the ocean-like Caspian crust to the southwest or the Paleo-Tethyan subduction, induced by the Zagros formation, to the northeast. Recently published studies suggest, on the contrary, that the northwest extrusion of the South Caspian region was accommodated by subduction beneath the north Caspian region to the north (Axen *et al*., 2001; Allen *et al*., 2002; Allen *et al*., 2003; Ritz *et al*., 2006; Hollinsworth *et al*., 2008).In addition, a number of studies on the geodynamic of the Paleo-Tethys demonstrate that Paleo-Tethys oceanic crust subducted northward from Late Devonian to Late Triassic time underneath the Turan Plate. On the other hand, Jaffaian *et al*, 2008 and Haghnazar *et al*, 2009, mentions, alkali basalt magmatism in central Alborz related to deep mantle melting and/ or mantle plume accompanied by crustal contamination in local extensional regime and/ or deep faults system. Alborz orogenic belt formed by continental- continental collision between the central Iranian block and the Eurasian plate (Vernant *et al*., 2004).therefore, Alborz region, exhibiting plateau morphology with an elevation 3000-5000 m above sea level. Geophysical studies have revealed that a mantle lithosphere is almost completely absent beneath the Alborz mountains (e.g., Sodoudi *et al*, 2009; Mirnejad *et al*, 2010). Bouguer anomaly modeling estimated crustal thickness of 35–40 km under the central Alborz and stimulated the idea of root deficiency (Dehghani and Makris, 1984). A relatively thicker crust (45–46 km) was shown for the same region based on surface wave analysis of a few events (Asudeh, 1982; Doloei and Roberts, 2003). The relatively thin crust for a 100 km wide, 3–5 km high mountain range has also been interpreted to be indicating lack of compensation by a lithospheric root (Guest *et al*., 2007).

Inadequate crustal root and the relatively thin lithosphere beneath the Alborz may imply that asthenospheric mantle is supporting the high elevation (Sodoudi *et al*., 2009). Absence of a crustal root in the Alborz may be due to lower crustal flow and sub-continental delamination as speculated by Allen *et al*, 2003; Mirnejad *et al*, 2010).

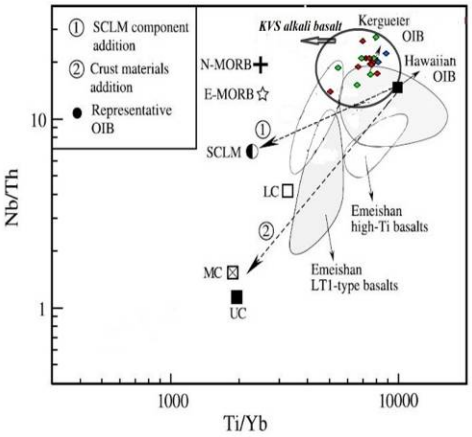

Fig. 12: Plot of Nb/Th vs. Ti/Yb for the KVF basalts, from Zhu *et al*.(2005) . Data for Hawaiian OIB are from Feigenson *et al*. (1996), Emeishan LT1, LT2-type and high-Ti basalts data are from Xiao *et al*. (2004). Note that all the KVF alkali basalt samples plot between Hawaiian OIB and sub-continental lithospheric mantle/lower crust, the lesser-contaminated samples plot toward the sub-continental lithospheric mantle and/or lower crus subcontinental lithospheric mantle (SCLM) values are from McDonough (1990); upper crust (UC), middle crust (MC) and lower crust (LC) values are from Rudnick and Gao, 2003.

Deep mantle melting and the delamination of sub-continental lithosphere in collision zone are explained by Lustrino (Lustrino, 2005). This model presented here is based on the role of lower crust and lithospheric mantle recycling by delamination and detachment. This process can explain at least some geochemical peculiarities of basaltic rocks found in large igneous provinces, as well as in small volume igneous activities, as well as in mid-ocean ridge basalts (Lustrino, 2005). Metamorphic reactions occurring in the lower continental crust as a consequence of continent–continent collision lead to a density increase (up to 3.8 g/cm3) with the appearance of garnet in the metamorphic assemblage (basalt amphibolites garnet clinopyroxenite/eclogite). This process leads to gravitative instability of the overthickened lithospheric keel (lower crust+ lithospheric mantle). This may detach from the uppermost lithosphere and sink into the upper mantle. Accordingly, metasomatic reactions between SiO2-rich lower crust partial melts and the uprising asthenospheric mantle (replacing the volume formerly occupied by the sunken lithospheric mantle and the lower crust) lead to formation of orthopyroxene-rich layers with strong crustal signatures.

In summary, major and trace element data,suggest that the KVF alkali basalts may have been derived from an OIB-type mantle source without major affecting to contribution subcontinental lithospheric mantle and/or lower crust. This study indicated that a huge piece of subcontinental lithospheric mantle (SCLM) and/ or lower crust of beneath Alborz mountain ranges has been delaminiated and detached from the upper crust in the past, which caused the thinning of lithosphere by graben structure and continental rifting. In general, isostatic relaxation follows regional shortening and thrust/nappe formation during continent-continent collision. The volume opened by the removal SCLM would be replaced by a new hot asthenospheric mantle plume. Melt and/ or fluid derivation from lower crust or SCLM could be hydrated and metasomatized mantle plume (Lustrino, 2005; Keskin, 2005). Therefore, adiabatic ascent and hydration of asthenospheric mantle cause melt derivation from asthenospheric mantle by decompressing of mantle. The variable degrees of partial melting (Fig. 12b) observed in the source of the KVF lavas are probably due to the pulsing influx of mantle plume material (Krientz *et al*, 2007).

Conclusion:

This study present new chemical data significant to our understanding of early cretaceous intraplate magmatism related to sub-continental lithospheric mantle delamination, asthenospheric mantle upwelling, graben structure, deep fault and local rift system in Kojor volcanic suite, central Alborz mountain ranges, North of Iran.

1. The KVF alkali basalts have domain rock type between olivine basalt to olivine trachy andesite and hypabbysal olivine dolerite.
2. The major and trace element composition of the KVF alkali basalts is controlled by fractional crystallization of olivine, plagioclase, Fe-Ti oxide ± clinopyroxene.
3. The major element variation and the REEs variability ratio of KVF alkali basalts, could be produced by decompressing of a garnet lherzolite mantle source and vary degrees of partial melting.

4. The KVF alkali basalts were derived from an OIB-type mantle source with discernable sub-continental lithospheric mantle sources and are generated from heterogeneous source with prominent geochemical heterogeneities.

REFERENCES

Allen, M., M.R. Ghassemi, M. Shahrabi, M. Qorashi, 2003. Accommodation of late Cenozoic oblique shortening in the Alborz range, northern Iran. Journal of Structural Geology, 25: 659-672.

Allen, M.B., S. Jones, A. Ismail-Zadeh, M. Simmons, L. Anderson, 2002. Onset of subduction as the cause of rapid Pliocene–Quaternary subsidence in the south Caspian basin. Geology, 30: 775-778.

Assereto, R., 1966a. The Jurassic Shemshak Formation in central Alborz (Iran). Rivista Italiana di Paleontologia e Stratigrafia., 72: 1133e1182.

Assereto, R., 1966b. Explanatory notes on the geological map of upper Djadjerud and Lar valleys (Central Alborz, Iran). In: Serie G., pubblicazione, 232. Istituto di Geologia, Universita` di Milano, Milano, Italy.

Asudeh, I., 1982. Seismic structure of Iran from surface and body wave data.Geophysical Journal Royal of Astronomy Society, 71: 715-730.

Axen, G.H., P.S. Lam, M. Grove, D.F. Stokli, J. Hassanzadeh, 2001. Exhumation of the west-central Alborz mountain, Iran: Caspian subsidence, and collision-related tectonics. Geology, 29: 559-562.

Besse, J., F. Torcq, Y. Gallet, L.E. Ricou, L. Krystyn, A. Saidi, 1998. Late Permian to Late Triassic palaeomagnetic data from Iran: constraints on the migration of the Iranian block through the Tethyan Ocean an initial destruction of Pangaea. Geophysical Journal International., 135: 77e92.

Boynton, W.V., 1984. Geochemistry of the rare earth elements: meteorite studies. In: Henderson P (ed) Rare earth element geochemistry. Elsevier, Amsterdam, pp: 63-114.

Clark, G.C., R.G. Davies, G. Hamzepour, C.R. Jones, 1975. Explanatory text of the Bandar-e-Pahlavi quadrangle map, 1:250,000. Geological Survey of Iran, Tehran, Iran, pp: 198.

Dehghani, G., J. Makris, 1984. The gravity field and crustal structure of Iran. Neues Jahrbuch für Geologie and Palaeontologie Abhundlungen., 168: 215-229.

Dicheng Zhu, A., A. Guitang Pan, B. Xuanxue Mo, A. Zhongli Liao, A. Xinsheng Jiang, A. Liquan Wang, Z. Zhidan, 2007. Petrogenesis of volcanic rocks in the Sangxiu Formation, central segment of Tethyan Himalaya: A probable example of plume–lithosphere interaction. Journal of Asian Earth Sciences, 29: 320-335.

Doloei, J., R. Roberts, 2003. Crust and uppermost mantle structure of Tehran region from analysis of teleseismic P-waveform receiver functions. Tectonophysics., 364: 115-133.

Fursich, F.T., M. Wilmsen, K. Seyed-Emami, F. Cecca, R. Majidifard, 2005. The upper Shemshak Formation (Toarcian-Aalenian) of the Eastern Alborz (Iran): Biota and palaeoenvironments during a transgressive-regressive cycle. Facies., 51: 365e384.

Gaetani, M., A. Arche, H. Kiersnowski, B. Chuvachov, S. Crasquin, M. Sandulescu, A. Seghedi, I. Zagorchev, A. Poisson, F. Hirsch, D. Vaslet, J. Le Metour, M. Ziegler, E. Abbate, L. Ait-Brahim, E. Barrier, S. Bouaziz, F. Bergerat, M.F. Brunet, J.P. Cadet, R. Stephenson, J.C. Guezou, A. Jabaloy, C. Lepvrier, G. Rimmele, 2000. Wordian paleogeographic map. In: Dercourt, J., Gaetani, M.,Vrielynck, B., Barrier, E., Biju-duval, B., Brunet, M.F., Cadet, J.P.,Crasquin, S., Sandulescu, M. (Eds.), Peri-Tethys Atlas and Explanatory Notes, Map 3. CCGM/CGMW, Paris, pp: 19e25.

Geological Survey of Iran, 1997. Balade. Geological Survey of Iran,Tehran, scale 1: 100,000.

Ghasemi-Nejad, E., A. Agha-Nabati, O. Dabiri, 2004. Late Triassic dinoflagellate cysts from the base of the Shemshak Group in north of Alborz Mountains, Iran. Review of Palaeobotany and Palynology, 132: 207e217.

Green, T.H., S.H. Sie, C.G. Ryan, D.R. Cousens, 1989. Proton microprobedetermined partitioning of Nb, Ta, Zr, Sr and Y between garnet, clinopyroxene and basaltic magma at high pressure and temperature. Chem Geol., 74: 201-216.

Guest, B., A. Guest, F. Axen, 2007. Late Tertiary tectonic evolution of northern Iran: a case for simple crustal folding. Global and Planetary Change, 58: 435-453.

Hagh Nazar, Sh., M. Vousughi Abedini, M. Poor Moafi, 2009. Petrology and Geochemistry of Mafic Rock in Javaher Dasht area, East of Gillan Province, North of Iran. PhD thesis in Shahid Beheshti University, pp: 298.

Hawkesworth, C.J., P.D. Kempton, N.W. Rogers, R.M. Ellam, P.W. Calsteren, 1990. Continental mantle lithosphere, and shallow level enrichment processes in the Earth's mantle. Earth and Planetary Science Letters 96, 256–268.

Hollinsworth, J., J. Jackson, R. Walker, H. Nazar, 2008. Extrusion tectonics and subduction in the eastern South Caspian region since 10 Ma. Geology, 36: 763-766.

Jaffarian, A., H. Emami, M. Vousughi Abedini, M. Ghaderi, 2009 Petrology and Geochemistry of Lower Paleozoic Magmatism in the East of Alborz. PhD thesis in IAUS, pp: 298.

Jenner, G.A., S.F. Foley, S.E. Jackson, T.H. Green, B.J. Fryer, H.P. Longerich, 1994. Determination of partition coefficients for trace elements in high pressure–temperature experimental run products by laser ablation microprobe-inductively coupled plasmamass spectrometry (LAM-ICP-MS). Geochim Cosmochim Acta., 58: 5099-5130.

Jenny, J., G. Stampfli, 1978. Lithostratigraphie du Permien de l'Elbourz oriental en Iran. Eclogae geologicae Helveticae., 71: 551e580.

Kaan, S.M., G. Cemal, 2009. Geochemistry of mafic rocks of the Karakaya complex, Turkey: evidence for plume-involvement in the Palaeotethyan extensional regime during the Middle and Late Triassic. Int J Earth Sci., 98: 367-385.

Keskin, M., 2005. Domal uplift and volcanism in a collision zone without a mantle plume: evidence from eastern Anatolia. MantlePlume.Org

Krienitz, M.S., K.M. Hasse, K. Mezger, M.A. Shaikh-Mashail, 2007. Magma genesis and mantle dynamic at the Harrat Ash Shaam volcanic field (South Syria). JOURNAL OF PETROLOGY 48: 1513-1542.

Le Bas, M.J., R.W. Le Maitre, A. Streckeisen, B.A. Zanettin, 1986. Chemical classification of volcanic rocks based on the total alkali-silica diagram. J Petrol., 27: 745-750.

Li, S.G., 1993. Ba–Nb–Th–La diagrams used to identify tectonic environments of ophiolite. Acta Petrologic Sinica 9: 146-157 (in Chinese with English abstract).

Li, X.H., Z.X. Li, H.W. Zhou, Y. Liu, P.D. Kinny, 2002. U–Pb zircon geochronology, geochemistry and Nd isotopic study of Neoproterozoic bimodal volcanic rocks in the Kangdian Rift of south China: implications for the initial rifting of Rodinia. Precambrian Research, 113: 135-154.

Liotard, J.M., J.M. Dautria, D. Bisch, J. Condomines, H. Mehdizadeh, J.F. Ritz, 2008. Origin of the absarokite–banakite association of the Damavand volcano (Iran): trace elements and Sr, Nd, Pb isotope constraints. International Journal of Earth Sciences, 97: 89-102.

Lustrino, M., 2005. How the Delamination and Detachment of Lower Crust Can Influence Basaltic Magmatism. Earth-Science Reviews.

McDonough, W.F. & S.S. Sun, 1995. The composition of the Earth Chemical Geology, 120: 223-253.

McDonough, W.F., 1990. Constraints on the composition of the continental lithospheric mantle. Earth and Planetary Science Letters, 101: 1-18.

McKenzie, D., 1989. Some remarks on the movement of small melt fractions in the mantle. Earth and Planetary Science Letters, 95: 53-72.

Mehdizadeh, H., J.M. Liotard, J.M. Dautria, 2002. Geochemical characteristics of an intracontinetnal shoshonitic association: the example of the Damavand volcano,Iran. Comptes Rendus Geoscience., 334: 111-117.

Menzies, M.A., C.J. Hawkesworth, 1987. Mantle Metasomatism. Academic Press, London.

Meschede, M., 1986. A method of discriminating between different type of mid-ocean ridge basalts and continental tholeiites with the Nb–Zr–Y diagram. Chemical Geology, 56: 207-218.

Mirnejad, H., J. Hassanzadeh, B.L. Cousens, B.E. Taylor, 2010 Geochemical evidence for deep mantle melting and lithospheric delamination as the origin of the inland Damavand volcanic rocks of northern Iran. Journal of Volcanology and Geothermal Research, 198: 288-296.

Nicholson, H., D. Latin, 1992. Olivine tholeiites from Krafla, Iceland:evidence for variation in melt fraction within a plume. J Petrol., 33: 1105-1124.

Pearce, J.A., 1980. REE values for various OIB etc. From lead isotope study of young volcanic rocks mid-oceanic ridges, oceanic islands and island arcs. Philos Trans R Soc Lond A 297: 409-445.

Pearce, J.A., M. Norry, 1979. Petrogenetic implications of Ti, Zr, Y and Nb variations in volcanic rocks. Contrib Mineral Petrol., 69: 33-47.

Hawkesworth, C.J., M.J. Norry, (Eds.), Continental Basalts and Mantle Xenoliths. Shiva, Nantwich, pp: 230-249.

Ritz, J.F., H. Nazar, A. Ghasemi, R. Salamati, A. Shafei, S. Solaymani, P. Vernant, 2006. Active transtension inside central Alborz: a new insight into northern Iran–southern Caspian geodynamics. Geology, 34: 477-480.

Rollinson, H.R., 1993. Using Geochemical Data: Evaluation, Presentation, Interpretation. Longman, New York, p: 352.

Rudnick, R.L., S. Gao, 2003. The composition of the continental crust.In: Rudnick, R.L. (Ed.), The Crust. In: Holland, H.D., Turekian, K.K.(Eds.), Treatise on Geochemistry, vol. 3. Elsevier, Oxford, pp: 1-64.

Ruttner, A.W., 1993. Southern borderland of Triassic Laurasia in north-east Iran. Geologische Rundschau, 82: 110e120.

Saidi, A., M.F. Brunet, L.E. Ricou, 1997. Continental accretion of the Iran Block to Eurasia as seen from Late Palaeozoic to early Cretaceous subsidence curves. Geodinamica Acta, 10: 189e208.

Seyed-Emami, K., 2003. Triassic in Iran. Facies 48, 95e106.Sengor, A.M.C., 1984. The Cimmeride orogenic system and the tectonics of Eurasia. Geological Society of America Special Publication, pp: 195: 82.

Shaw, J., 2003. Geochemistry of Cenozoic volcanism and Arabian lithospheric mantle in Jordan. Ph.D. thesis, Royal Holloway University of London, pp: 268.

Sodoudi, F., X. Yuan, R. Kind, B. Heit, A. Sadidkhouy, 2009. Evidence for a missing crustal root and a thin lithosphere beneath the Central Alborz by receiver function studies. Geophysics Journal International., 177: 733-742.

Spath, A., A.P. Le Roex, R.A. Duncan, 1996. The geochemistry of lavas from the Comores Archipelago, Western Indian Ocean: petrogenesis and mantle source region characteristics. J Petrol., 37: 961-991.

Stampfli, G., J. Marcoux, A. Baud, 1991. Tethyan margins in space and time. Palaeogeography, Palaeoclimatology and Palaeoecology, 87.

Stampfli, G.M., G.D. Borel, 2002. A plate tectonic model for the Palaeozoic and Mesozoic constrained by dynamic plate boundaries and restored synthetic oceanic isochrones. Earth Planetary Sciences Letters, 196: 17e33.

Stocklin, J., 1974. Possible ancient continental margins in Iran. In: Burk, C.A.,Drake, C.L. (Eds.), The Geology of Continental Margins. Springer, Berlin, pp: 873e887.

Sun, S.S., W.F. McDonough, 1989. Chemical and isotopic systematics of oceanic basalts: implications for mantle composition and processes. In: Saunders AD, Norry MJ (eds) Magmatism in the ocean basins. Geol Soc Spec Publ., 42: 313-345.

Tainton, K.M., D. McKenzie, 1994. The generation of kimberlites, lamproites and their source rocks. Journal of Petrology, 35: 787-817.

Taki, S., A. Darvishzadeh, M. Ghaderi, 2009. Petrology of Igneous Rocks in Deylaman Area, Central Alborz. PhD thesis in IAUS, pp: 272.

Tatar, M., D. Hatzfeld, J. Martinod, A. Walpersdorf, M. Ghafori-Ashtiany, J. Chery, 2002. The present-day deformation of the central Zagros from GPS measurements. Geophysical Research Letters, 29(19): 1927, doi:10.1029/2002GL015427.

Vernant, P., F. Nilforoushan, J. Che´ry, R. Bayer, Y. Djamour, F. Masson, H. Nankali, J.-F. Ritz, M. Sedighi, F. Tavakoli, 2004. Deciphering oblique shortening of central Alborz in Iran using geodetic data. Earth andPlanetary Science Letters, 223: 177e185.

Weinstaein, Y., O. Navon, R. Altherr, M. Stein, 2006. The Role of Lithospheric Mantle Heterogeneity in the Generation of Plio-Pleistocene Alkali Basaltic Suites from NW Harrat Ash Shaam (Israel). JOURNAL OF PETROLOGY, 47: 1017-1050.

Weinstein, Y., O. Navon, & B. Lang, 1994. Fractionation of Pleistocene alkali-basalts from the northern Golan Heights, Israel .Israel Journal of Earth Sciences, 43: 63-79.

Wilson, M., 1989. Igneous Petrogenesis. A Global Tectonic Approach. Chapman and Hall, UK.

Winchester, J.A., P.A. Floyd, 1977. Geochemical discrimination of different magma series and their differentiation products using immobile elements. Chemical Geology, 20: 325-342.

Xiao, L., Y.G. Xu, H.J. Mei, Y.F. Zheng, B. He, Pirajno, Franco, 2004.Distinct mantle sources of low-Ti and high-Ti basalts from the western Emeishan large igneous province, SW China: implications for plume lithosphere interaction. Earth and Planetary Science Letters, 228: 525-546.

Zanchi, A., F. Berra, M. Mattei, M.R. Ghassemi, J. Sabouri, 2006. Inversion tectonics in central Alborz, Iran. Journal of Structural Geology, 28: 2023-2037.

Zhu, D.C., G.T. Pan, X.X. Mo, L.Q. Wang, Z.L. Liao, X.S. Jiang, Q.R. Geng, 2005. SHRIMP U–Pb zircon dating for the dacite of the Sangxiu formation in the central segment of Tethyan Himalaya and its implications. Chinese Science Bulletin., 50: 563-568.